

Asymmetrical Reciprocity-based Federated Learning for Resolving Disparities in Medical Diagnosis

Jiaqi Wang*
The Pennsylvania State University
University Park, PA, USA
jqwang@psu.edu

Ziyi Yin*
The Pennsylvania State University
University Park, PA, USA
zmy5171@psu.edu

Quanzeng You
ByteDance
Bellevue, WA, USA
quanzeng.you@outlook.com

Lingjuan Lyu
Sony AI
Zurich, Switzerland
Lingjuan.Lv@sony.com

Fenglong Ma
The Pennsylvania State University
University Park, PA, USA
fenglong@psu.edu

Abstract

Geographic health disparities pose a pressing global challenge, particularly in underserved regions of low- and middle-income nations. Addressing this issue requires a collaborative approach to enhance healthcare quality, leveraging support from medically more developed areas. Federated learning emerges as a promising tool for this purpose. However, the scarcity of medical data and limited computation resources in underserved regions make collaborative training of powerful machine learning models challenging. Furthermore, there exists an asymmetrical reciprocity between underserved and developed regions. To overcome these challenges, we propose a novel cross-silo federated learning framework, named FedHelp, aimed at alleviating geographic health disparities and fortifying the diagnostic capabilities of underserved regions. Specifically, FedHelp leverages foundational model knowledge via one-time API access to guide the learning process of underserved small clients, addressing the challenge of insufficient data. Additionally, we introduce a novel asymmetric dual knowledge distillation module to manage the issue of asymmetric reciprocity, facilitating the exchange of necessary knowledge between developed large clients and underserved small clients. We validate the effectiveness and utility of FedHelp through extensive experiments on both medical image classification and segmentation tasks. The experimental results demonstrate significant performance improvement compared to state-of-the-art baselines, particularly benefiting clients in underserved regions.

CCS Concepts

• **Applied computing** → **Health informatics**; • **Computing methodologies** → *Federated learning*; *Artificial intelligence*.

*These authors contributed equally to this work.

Permission to make digital or hard copies of all or part of this work for personal or classroom use is granted without fee provided that copies are not made or distributed for profit or commercial advantage and that copies bear this notice and the full citation on the first page. Copyrights for components of this work owned by others than the author(s) must be honored. Abstracting with credit is permitted. To copy otherwise, or republish, to post on servers or to redistribute to lists, requires prior specific permission and/or a fee. Request permissions from permissions@acm.org.

KDD '25, August 3–7, 2025, Toronto, ON, Canada

© 2025 Copyright held by the owner/author(s). Publication rights licensed to ACM.
ACM ISBN 979-8-4007-1245-6/25/08
<https://doi.org/10.1145/3690624.3709235>

Keywords

Federated Learning, Healthcare Disparity, Medical Diagnosis

ACM Reference Format:

Jiaqi Wang*, Ziyi Yin*, Quanzeng You, Lingjuan Lyu, and Fenglong Ma. 2025. Asymmetrical Reciprocity-based Federated Learning for Resolving Disparities in Medical Diagnosis. In *Proceedings of the 31st ACM SIGKDD Conference on Knowledge Discovery and Data Mining V.1 (KDD '25)*, August 3–7, 2025, Toronto, ON, Canada. ACM, New York, NY, USA, 12 pages. <https://doi.org/10.1145/3690624.3709235>

1 Introduction

Geographic health disparities pose a fundamental challenge to countries worldwide [4, 22, 30, 47]. These disparities underscore the unequal distribution of health resources, access to healthcare services, and health outcomes across different geographic regions. Particularly in low- and middle-income nations, rural areas often grapple with significant challenges related to healthcare infrastructure, access to medical professionals, and essential health services [1, 46]. This lack of access can result in higher rates of preventable diseases, maternal and child mortality, and overall poorer health outcomes in these regions. Furthermore, factors such as limited funding, lack of education, and a shortage of expertise in rural areas hinder their ability to invest in cutting-edge technologies. Consequently, *finding collaborative ways to enhance healthcare quality in underserved regions with the support of medically developed areas is an urgent and essential social issue.*

Federated learning, a technique widely employed in the medical domain, presents a potential solution to this challenge by enabling collaborative training of robust machine learning models without centralizing healthcare data [11, 16, 18, 23, 24, 35, 38, 39, 48]. However, many existing approaches necessitate clients to employ identical models, a requirement unsuitable for our context where underserved regions face economic constraints in procuring high-cost computational resources. In essence, these regions or clients can only afford small-sized models. In contrast, medically developed areas typically utilize large models, thereby resulting in the challenge of *heterogeneous models* in federated learning. While numerous strategies [8, 9, 15, 19, 21, 41, 49, 50] have been proposed to tackle the challenges posed by heterogeneous federated learning, these approaches still suffer from the following challenges:

• **C1: Limited medical data in underserved regions.** Several factors, including inadequate access to healthcare facilities, a lack of

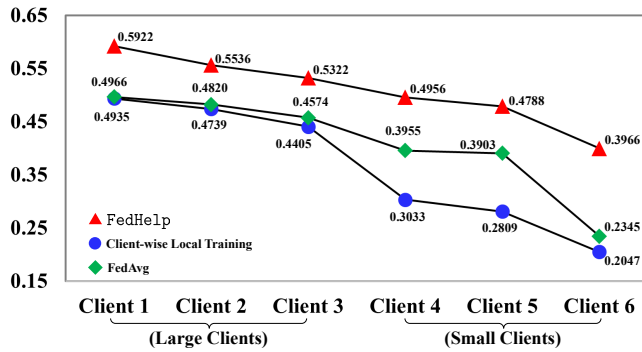


Figure 1: Client accuracy comparison between client-wise local training, FedAvg, and the proposed FedHelp on the Fed-ISIS19 dataset. The size of each client can be found in Section 4.2.

awareness regarding the importance of medical record-keeping, and insufficient technology for maintaining electronic health records, contribute to the scarcity of medical data in underserved regions. In our federated learning framework, each region is treated as a client. As depicted in Figure 1, small clients typically exhibit significantly lower performance than larger ones in local training. While applying the existing federated learning algorithm FedAvg [23] does improve performance, the benefits are primarily observed in clients with relatively small datasets (clients 4 and 5), excluding both the largest and smallest ones. Consequently, it is crucial to explore new learning strategies that can benefit **ALL** clients in our setting. Without such inclusive approaches, there is little incentive for medically developed large clients to contribute to the improvement of underserved small clients.

- **C2: Asymmetrical reciprocity among clients.** Traditional federated learning methodologies treat all clients equally, aiming to collaboratively train a shared global model or personalized client models. However, this study deviates from the norm by focusing on harnessing the abundant resources of medically developed areas to enhance the diagnostic performance of underserved regions using compact models without the need to share their data. In essence, the small clients emerge as the primary beneficiaries. While large clients can gain insights from small client information through model aggregation, they still act as valuable resource providers. Thus, the collaboration in this scenario exhibits asymmetric reciprocity among clients, which aligns with our observations in Figure 1. However, effectively modeling this asymmetric reciprocity poses a novel challenge in federated learning.

To tackle these challenges simultaneously, we introduce a groundbreaking cross-silo **f**ederated learning framework called FedHelp¹, specifically tailored to combat geographic **h**ealth disparities and bolster the diagnostic capabilities of underserved regions, as illustrated in Figure 2. To tackle the first challenge (C1) encountered during the training of small clients, we advocate harnessing knowledge from foundational models [54] via only one-time API access using public data rather than private medical data in Section 3.2. This acquired knowledge serves as a guiding light in training small surrogate models in Section 3.3. Meanwhile, the

¹The source code is available at <https://github.com/JackqqWang/fedhelp>.

second challenge (C2) arises when training large clients. To circumvent escalating communication costs, we advocate distilling a proxy model for each large client, mirroring the network structure of small clients. This proxy model acts as an intermediary, facilitating the exchange of information between large and small clients. Specifically, we have devised an innovative asymmetrical dual knowledge distillation strategy to address the challenge of asymmetrical reciprocity in Section 3.4. Subsequently, the small surrogate and proxy models are uploaded to the server for aggregation in Section 3.5.

To the best of our knowledge, this is the first work to leverage federated learning techniques to mitigate the global issue of geographic health disparities, thereby augmenting healthcare quality in underserved regions. In particular, we introduce a unique framework, FedHelp, designed to address the challenge of small data through accessing expansive foundation models via API in an efficient way and tackle the distinctive hurdle of asymmetrical reciprocity via the proposed dual knowledge distillation strategy. We conduct comprehensive experiments encompassing multi-class and binary medical image classification tasks as well as 2D and 3D semantic segmentation tasks, comparing the results with state-of-the-art baselines. The experimental outcomes unequivocally affirm the efficacy of the FedHelp framework.

2 Related Work

2.1 Federated Learning

Federated learning [2, 23, 53], aiming to collaboratively train a machine learning model without sharing clients' private data, has been applied to the medical domain [11, 18, 38, 38–40, 45, 48]. Compared with traditional federated learning frameworks [16, 23, 24, 35], personalized federated learning focuses on the performance of the local clients [6, 32, 34, 52], achieving superior performance. However, either traditional federated learning or personalized federated learning models require that all the clients share the identical model structure. Though several heterogeneous federated learning frameworks [8, 9, 15, 21, 37, 42, 49, 50] have been proposed to solve this issue, they are not typically designed to address the challenges in the medical domain. While one recent medical-related work ProxyFL [12] proposes a decentralized federated learning method with each client managing a small model, it neglects the essential distinctions between private and proxy models. Moreover, this decentralized approach leads to increased communication expenses.

2.2 Dual Knowledge Distillation

Knowledge distillation [7] treats the large model as a teacher, which passes knowledge to a small student model to enhance its performance. The most relevant work is bidirectional or dual knowledge distillation [14], enabling the teacher and student to learn knowledge from each other. In [14, 28], the bidirectional distillation technique is utilized to solve the top-k ranking research problem and machine translation [10, 51, 55]. Although a few studies apply bidirectional knowledge distillation in federated learning to conduct the tasks of distracted driving detection [31], medical relation extraction [33], and the IoT system [26], they all treat both teacher and student models equally yet ignore the importance of asymmetrical reciprocity.

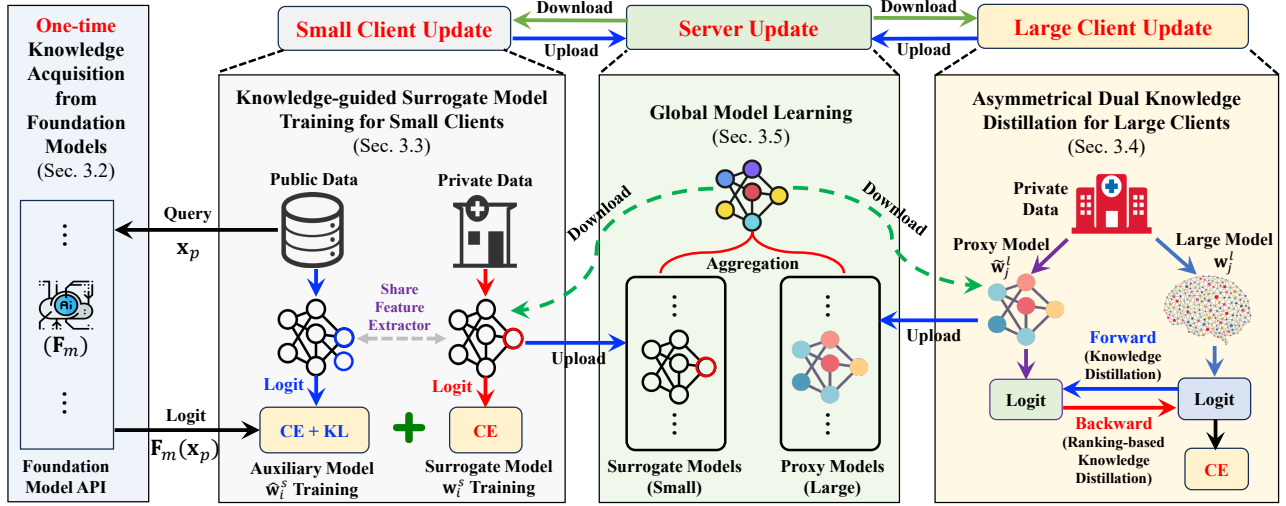


Figure 2: Overview of the proposed FedHeP framework. “CE”/“KL” denotes the cross-entropy loss/Kullback–Leibler divergence.

FedType [43] is the most relevant work, addressing the asymmetrical reciprocity between small proxy models and large client models. However, our model, FedHeP, differs from FedType in several key aspects. First, the approach to calculating loss values is fundamentally different. FedType relies on training two conformal models to estimate uncertainty sets—one for the large client model and another for the proxy model. This process introduces additional computational overhead and requires tuning more hyperparameters. In contrast, FedHeP adopts a more straightforward strategy by directly leveraging logit ranks to select top classes, eliminating the need for extra conformal models. Second, FedHeP employs a distinct loss function specifically designed for small clients, as described in Eq. (3), to address challenges such as small data sizes and low data quality. FedType, on the other hand, applies the same loss function uniformly across all clients, disregarding these specific challenges. This fundamental difference highlights the adaptability of FedHeP to heterogeneous client conditions.

3 Methodology

3.1 Model Overview

The goal of this work is to enable the training of federated learning under the settings of clients with different capacities. Let $C^s = \{C_1^s, \dots, C_{N_s}^s\}$ be the small client set in underserved regions, where N_s represents the number of small clients. Let $C^l = \{C_1^l, \dots, C_{N_l}^l\}$ denote the large client set, where N_l denotes the number of large clients. Each client stores a training dataset \mathcal{D}_i^s for a small client or \mathcal{D}_j^l for a large client. In our setting, the size of \mathcal{D}_j^l is far greater than that of \mathcal{D}_i^s . To increase the diagnostic ability of small clients, we propose a novel yet general framework FedHeP consisting of three key components: knowledge acquisition, small client training, large client training, and global model learning, in Figure 2.

The knowledge acquisition module aims to generate logits or probability distributions from M foundation models $\{F_1, \dots, F_M\}$ for public data \mathcal{D}_p , which are further used to guide the learning of

clients. Note that the public data, including their image types and labels, may differ from those stored on clients. For small clients, we design a new knowledge-guided surrogate training strategy to handle the issue of data insufficiency. Since the large clients hold high-quality and plenty of training data, we propose a novel asymmetrical dual knowledge distillation technique to distill large client models and lightweight proxy models. The lightweight models from both small and large clients will be uploaded to the server for global model learning. Next, we use the medical image classification task as an example and provide the details of each component.

3.2 One-time Knowledge Acquisition from Foundation Models

It is well-known that foundation models [5, 27] usually outperform basic deep learning models on many tasks due to their large capacity. Unfortunately, more and more such models are packed as application programming interfaces (APIs) and not open-sourced like GPT-4. An ideal way to use these APIs is to directly upload a small set of data to their cloud servers, which helps us to fine-tune customized models and return them to users. However, in our setting, medical data are extremely sensitive and cannot be sent to third parties. Thus, it is challenging to obtain customized models without sharing private medical data.

To solve this challenge, we acquire knowledge from large foundation models with the help of public data \mathcal{D}_p , where all clients can access them. Assume that all the clients can also access the APIs of foundation models $\{F_1, \dots, F_M\}$ and request the probability distributions for the public data. The returned probability distributions will be treated as knowledge for guiding the clients’ training.

3.3 Small Clients: Knowledge-guided Surrogate Model Training

In our setting, each small client can be treated as a rural emergency hospital holding a small set of data \mathcal{D}_i^s without sufficient computational resources to train a sizeable yet accurate deep learning model.

To solve this issue, we propose to use the knowledge returned from public APIs as guidance to help the model training. *It should be emphasized that our model leverages foundation models exclusively through one-time API access during the initial phase of federated learning. This approach eliminates the need for deploying these models individually across each smaller client and does not involve them directly in the learning processes.*

Our general setting allows the accessible public data \mathcal{D}_p to be different from the private data \mathcal{D}_i^s . Thus, the client model \mathbf{w}_i^s cannot be directly used for training \mathcal{D}_p . To address this problem, we propose to introduce an auxiliary model $\hat{\mathbf{w}}_i^s$ for training on public data. $\hat{\mathbf{w}}_i^s$ shares the same feature extraction layers with the client model \mathbf{w}_i^s , which can be seen as a surrogate model of large foundation models. The only difference between $\hat{\mathbf{w}}_i^s$ and \mathbf{w}_i^s is the classification layer that handles diverse data distribution.

Specifically, FedHeIp first queries an API $F_m \in \{F_1, \dots, F_M\}$ for each public data $x_p \in \mathcal{D}_p$, which returns a label distribution $F_m(x_p)$. These returned distributions from M APIs are used as guidance in surrogate model training via the following loss:

$$\mathcal{R}_i^s = \sum_{p=1}^P [\text{CE}(\hat{\mathbf{w}}_i^s(x_p), y_p) + \lambda_R \text{KL}(\sum_{m=1}^M \alpha_{i,p}^m F_m(x_p) || \hat{\mathbf{w}}_i^s(x_p))], \quad (1)$$

where P is the number of public data, $\text{CE}(\cdot, \cdot)$ is the cross-entropy loss, and $\text{KL}(\cdot, \cdot)$ is the Kullback–Leibler divergence. λ_R is the hyperparameter. $\alpha_{i,p}^m$ denotes the learned contribution score of each API on each public data, and $\sum_{m=1}^M \alpha_{i,p}^m = 1$.

FedHeIp then trains the surrogate model $\hat{\mathbf{w}}_i^s$ using the client private data \mathcal{D}_i^s with the cross-entropy loss as follows:

$$\mathcal{L}_i^s = \sum_{k=1}^{K_i^s} \text{CE}(\mathbf{w}_i^s(\mathbf{x}_k^{s,i}), \mathbf{y}_k^{s,i}), \quad (2)$$

where K_i^s is the number of data in \mathcal{D}_i^s . Since $\hat{\mathbf{w}}_i^s$ and \mathbf{w}_i^s share the same feature extractor, we use a joint optimization approach by jointly optimizing \mathcal{R}_i^s and \mathcal{L}_i^s simultaneously via

$$\mathcal{J}_i^s = \mathcal{L}_i^s + \lambda_J \mathcal{R}_i^s, \quad (3)$$

where λ_J is a trade-off parameter.

3.4 Large Clients: Asymmetrical Dual Knowledge Distillation

Different from small clients, large clients have sufficient data and computation resources to train complex deep learning models. Thus, it is unnecessary to utilize public data as small clients do, avoiding introducing noise during model training due to the different data distributions. However, uploading and downloading these large models consume a large amount of communication. To make the whole system more communication-efficient, we propose to distill small proxy models for these clients, which are further used in global model learning.

Intuitively, the large capacity and strong predictive ability of the large model \mathbf{w}_j^l allows it to distill a small, powerful proxy model $\tilde{\mathbf{w}}_j^l$ with traditional knowledge distillation techniques. The large model \mathbf{w}_j^l can be treated as a teacher, and the proxy model $\tilde{\mathbf{w}}_j^l$ can be seen as a student. However, such a simple approach aims to learn effective student models but ignores the importance of the proxy model.

In fact, the proxy model $\tilde{\mathbf{w}}_j^l$ contains two kinds of information. The first part is from the forward knowledge distillation, and the second is from other clients via the global model aggregation, which can be found in Section 3.5. In other words, $\tilde{\mathbf{w}}_j^l$ carries diverse critical information aggregated from small clients $C^s = \{C_1^s, \dots, C_{N_s}^s\}$ and other large clients $C_{\neq j}^l = \{C_1^l, \dots, C_{j-1}^l, C_{j+1}^l, \dots, C_{N_l}^l\}$.

To tackle this issue, we design a novel asymmetrical dual knowledge distillation strategy, which enables the transfer of information in a bidirectional way – *forward* and *backward*. The **forward** direction allows the information transfer from the large model \mathbf{w}_j^l to the proxy model $\tilde{\mathbf{w}}_j^l$ with traditional knowledge distillation as follows:

$$\overrightarrow{\mathcal{KD}}_j^l = \sum_{k=1}^{K_j^l} \text{KL}(\mathbf{w}_j^l(\mathbf{x}_k^{l,j}) || \tilde{\mathbf{w}}_j^l(\mathbf{x}_k^{l,j})), \quad (4)$$

where K_j^l is the number of data in \mathcal{D}_j^l . Since the large model \mathbf{w}_j^l is usually more powerful than the proxy one $\tilde{\mathbf{w}}_j^l$, mandatorily distilling knowledge from $\tilde{\mathbf{w}}_j^l$ to \mathbf{w}_j^l in the **backward** direction will introduce noise for the large model training. To address this problem, we propose a ranking-based knowledge distillation to imitate the *behavior* of the proxy model for the large model.

Intuitively, if the behaviors of the two models are similar, their prediction logits should also be similar. To avoid introducing extra noise by forcing the large model’s logits to be similar to those of small ones, we propose to use the value rank of classes in the logits to imitate behaviors. The ranks only exhibit the relative magnitude of probabilities instead of real values, which can be treated as a loose constraint.

Specifically, for a given data $\mathbf{x}_k^{l,j}$, the proxy model $\tilde{\mathbf{w}}_j^l$ can generate a logit or a class probability distribution $\tilde{\mathbf{w}}_j^l(\mathbf{x}_k^{l,j})$. Since our goal is to transfer the diversity information from the proxy model to the large one and avoid introducing too much extra information, in our proposed RKD, we only focus on the top-ranked classes in $\tilde{\mathbf{w}}_j^l(\mathbf{x}_k^{l,j})$. To make the large model imitate the behavior of the proxy model, we enforce to improve the ranks of these top classes in $\mathbf{w}_j^l(\mathbf{x}_k^{l,j})$ using the following loss:

$$\overleftarrow{\mathcal{KD}}_j^l = - \sum_{k=1}^{K_j^l} \sum_{r \in \Omega} \log\left(\frac{\exp(\mathbf{w}_j^l(\mathbf{x}_k^{l,j})[r])}{\Phi}\right), \quad (5)$$

$$\Phi = \sum_{u \in \Omega} \exp(\mathbf{w}_j^l(\mathbf{x}_k^{l,j})[u]) + \sum_{v \in \Omega'} \exp(\mathbf{w}_j^l(\mathbf{x}_k^{l,j})[v]), \quad (6)$$

where Ω denotes the top-ranked class indexes, and Ω' represents the remaining classes. Note that the only function of Eq. (5) is to use the top class ranks Ω generated by the proxy model to guide the improvement of the corresponding class probabilities learned by the large model. This constraint relaxes the hard constraint of the traditional knowledge installation and enables the large model to imitate the behaviors of the proxy model.

FedHeIp can also train the large model $\mathbf{w}_j^l(\mathbf{x}_k^{l,j})$ using the labeled dataset \mathcal{D}_j^l with the cross-entropy loss \mathcal{L}_j^l , similar to Eq. (2). Finally, the loss function for training large clients is defined as follows:

$$\mathcal{G}_j^l = \mathcal{L}_j^l + \lambda_F \overrightarrow{\mathcal{KD}}_j^l + \lambda_B \overleftarrow{\mathcal{KD}}_j^l, \quad (7)$$

Table 1: Accuracy comparison on the Fed-ISIC19 dataset. “Underline” indicates the best baseline performance, and “bold” denotes the best performance. “% imp.” is the value of percentage improvement compared with the best baseline.

Setting	Model	Large			Small			Client Average
		Client 1	Client 2	Client 3	Client 4	Client 5	Client 6	
Homo.	FedAvg	0.4966	0.4820	0.4574	0.3955	0.3903	0.2345	0.4094
	FedProx	0.4895	0.4871	0.4612	0.4086	0.4015	0.2411	0.4148
	Per-FedAvg	0.5093	0.4903	0.4689	0.4126	0.4087	0.2456	0.4226
	PFedMe	0.5144	0.5066	0.4707	0.4233	0.4153	0.2508	0.4302
	PFedBayes	<u>0.5365</u>	<u>0.5207</u>	<u>0.4876</u>	<u>0.4278</u>	<u>0.4222</u>	<u>0.2688</u>	<u>0.4439</u>
Hete.	FedMD	0.5248	0.5122	0.4603	0.4139	0.4005	<u>0.2718</u>	0.4306
	FedGH	0.5286	0.5014	0.4755	0.4184	0.4011	0.2641	0.4315
	FedKEAF	0.5101	0.4979	0.4668	0.4096	0.4121	0.2669	0.4272
	FCCL	0.5175	0.4961	0.4614	0.4107	<u>0.4248</u>	0.2715	0.4303
	FedHelp (% imp.)	0.5922 10.38%↑	0.5563 6.84%↑	0.5322 9.15%↑	0.4956 15.85%↑	0.4788 12.71%↑	0.3996 47.02%↑	0.5091 14.69%↑

where λ_F and λ_B are hyperparameters. In our setting, we only need the proxy models to have the same network structure, but the network structures of large client models can be different, which increases the generalization ability of the proposed framework.

3.5 Global Model Learning

The surrogate models $\{\mathbf{w}_1^s, \dots, \mathbf{w}_{N_s}^s\}$ from small clients and the proxy models $\{\hat{\mathbf{w}}_1^l, \dots, \hat{\mathbf{w}}_{N_l}^l\}$ from large clients will be uploaded to the server to exchange parameter information. Since these models have identical network structures, we can use any existing model aggregation approaches, such as FedAvg [23], to learn the global model. The global model will be distributed to each client for the iterative update until FedHelp converges. Note that the proposed FedHelp is a general framework and can also be used for other tasks, such as the medical image segmentation task, and the details can be found in **Appendix A**. Besides, the whole training procedure of the proposed FedHelp can be found in **Appendix B**.

4 Medical Image Classification

In this section, we validate the proposed FedHelp on the three medical image classification tasks, including a **multiclass** melanoma classification and a **binary** pneumonia classification using chest x-rays.

4.1 Experimental Settings

4.1.1 Baselines. In our setting, clients are divided into large and small clients. Thus, this is a heterogeneous federated learning scenario. Small clients use ResNet20 as their model, while large clients use ResNet110. To fairly evaluate the performance of the proposed FedHelp, we employ two sets of baselines:

- **Homogeneous** baselines are traditional federated learning models, including FedAvg [23], FedProx [17], Per-FedAvg [6], PFedMe [34], and PFedBayes [52], which employ the small model ResNet20 as the client model.
- **Heterogeneous** baselines include FedMD [15], FedGH [49], FedKEAF [50], and FCCL [8]. They use both ResNet110 for

large clients and ResNet20 for small clients and use the public data \mathcal{D}_p as a part of model input.

Note that we do not list pFedHR [41] as a baseline since it maintains a personalized model for each client on the server. However, FedHelp and baselines do not have such a constraint. The details of each model and its implementation can be found in **Appendix C**.

4.1.2 Implementation. For the medical image classification task, we employ two foundation models trained on CLIP [27], including ViT-L/14 [5] and RN50x16 [27]². The public dataset \mathcal{D}_p is CIFAR-100 [13], and the number of public data is 10,000. The proxy model is ResNet20. We set $\lambda_R = 0.1$, $\lambda_J = 0.2$, $\lambda_F = 1$, and $\lambda_B = 0.2$. We use accuracy Ω in Eq. (5) as 3 for multi-class classification and 1 for binary classification. With the early stopping mechanism, we set the maximum communication rounds to 100. Furthermore, our proposed model offers flexibility in the choice of public datasets. In our main results, we utilize CIFAR-100, a non-medical dataset. In Sec. 4.4, we present results from the medical public dataset NCT-CRC-HE-100K.

4.2 Melanoma Classification

The Fed-ISIC19³ dataset [3, 25, 36], consisting of 23,247 dermoscopy images, is used to classify eight different types of melanoma. Using the data partition of FLamby [25], we divide the six clients into three large and three small ones, where the number of training/testing data is 9,930/2,483, 3,163/791, 2,690/673, 655/164, 351/88, and 180/45, respectively. The cross-silo setting requires all clients to be involved in training at each communication round.

4.2.1 Performance Comparison. Table 1 displays the experimental findings on the Fed-ISIC19 dataset. Notably, our proposed FedHelp outperforms all baseline models, particularly showcasing remarkable improvement on small clients. For the smallest client, the observed percentage improvement is substantial, reaching up to 47.1%.

²We selected these two models to simulate foundation model APIs as they were pretrained on the CIFAR-100 dataset, which serves as the public data in the medical image classification experiment.

³The links of the datasets used in the experiments can be found in **Appendix D**.

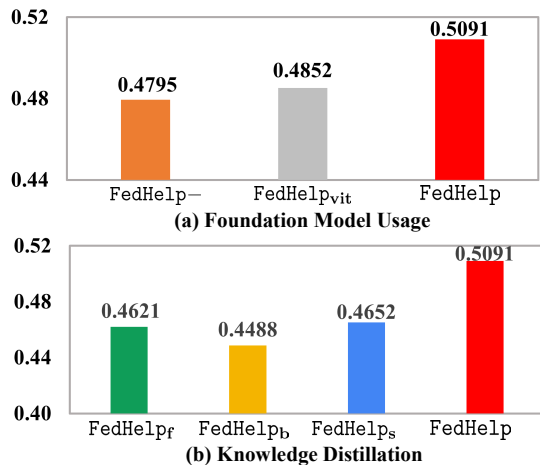


Figure 3: Average client accuracy of two ablation studies on melanoma classification

Additionally, a consistent trend is observed across all approaches, indicating better performance on large clients compared to their smaller counterparts. This aligns with expectations, as larger clients inherently possess more data and even employ larger models, as seen in the heterogeneous baselines.

Although heterogeneous baselines leverage larger client models and incorporate additional public data, their performance remains comparable to most homogeneous models. This observation underscores that the aggregation approaches of heterogeneous models might not be well-suited for our setting, potentially due to small clients impeding the learning progress of large clients.

In contrast to all other approaches, our proposed FedHelp not only integrates foundation models to enhance the learning of small clients but also introduces a novel asymmetric dual knowledge distillation method to boost the learning of large clients. As a result, it achieves the highest performance. These results unequivocally demonstrate the effectiveness of the proposed FedHelp.

4.2.2 Ablation Study. We conduct two experiments to assess the effectiveness of our model design.

(1) **Knowledge Enhancement with Foundation Models** (Section 3.3). Given the integration of two foundation model APIs to enhance the learning of small clients, the first ablation study aims to validate the utility of these APIs. Two baselines are employed for comparison: The first baseline, denoted as FedHelp-, indicates the absence of any APIs, while the remaining components are identical to FedHelp. FedHelp_{vit} signifies the utilization of only one API, ViT, during the small client learning process. The results are shown in Figure 3 (a). Our observations show that both FedHelp_{vit} and FedHelp outperform FedHelp-, indicating that the incorporation of foundation models is beneficial for enhancing the training of small clients. Furthermore, a positive correlation between the number of APIs and performance is evident when comparing FedHelp_{vit} and FedHelp. Notably, even when removing all APIs (FedHelp-), the drop in performance is smaller than the increase observed in Table 1. This result confirms that the primary performance improvement

Table 2: Average of 3 epoch training time (in seconds) on the Fed-ISIC19 dataset.

Setting	Time(s)
Training small clients with FedHelp	275.67
Training small clients only using the CE loss	251.00
Training large models with FedHelp	511.67
Training large models only using the CE loss	434.00
Training large models with the BKD loss	479.67

stems from the designed asymmetric dual knowledge distillation, rather than the use of foundation model APIs.

(2) **Asymmetric Dual Knowledge Distillation** (Section 3.4). In our model design, we propose a novel asymmetric dual knowledge distillation approach to benefit the learning of both small and large clients. We use three baselines in this ablation study to validate the effectiveness of the proposed strategy, including one-directional knowledge distillation methods (i.e., FedHelp_f (forward) and FedHelp_b (backward)) and a symmetric dual knowledge distillation approach FedHelp_s. The results are shown in Figure 3 (b). These results suggest that the three distillation approaches are not optimal for our setting. Solely employing forward knowledge distillation (FedHelp_f) effectively guides the learning of small models, but the transfer of knowledge from small to large models is lacking. Conversely, the outcome of FedHelp_b indicates a potential lag in small model training compared to large model training, despite the inclusion of diverse information. Notably, even when using FedHelp_b, the foundation model APIs enhance our model’s performance beyond the best baseline, as shown in Table 1. In contrast, traditional dual knowledge distillation (FedHelp_s) outperforms both FedHelp_f and FedHelp_b, emphasizing the importance of exchanging knowledge between large and small clients. However, it highlights the need for a well-designed approach to model knowledge transfer from small to large clients.

4.2.3 Resource Usage Analysis. Previous experiments have unequivocally illustrated the efficacy of our proposed approach, FedHelp. Nevertheless, leveraging the logits from public data for small client training and integrating asymmetrical reciprocity learning for large clients could further optimize resource utilization. This experiment aims to quantitatively assess resource consumption by scrutinizing both computation and communication costs.

(1) **Computation Costs.** Training time is a quantitative metric for assessing the efficiency of different approaches. In this experiment, we calculate the average training time across three epochs for various methods, with the results presented in Table 2. Here, “BKD” denotes the utilization of symmetric knowledge distillation during model training. Analysis reveals that the training time for FedHelp surpasses that of baseline methods for both large and small clients. Nevertheless, the incremental training time is moderate, representing a 6.67% increase compared to the large client using the BKD loss and a 9.83% extension relative to the small client using the CE loss. Despite this, our approach demonstrates substantial performance enhancements, particularly for small clients, showcasing an improvement of up to 47.02%, as illustrated in Table 1. Importantly,

Table 3: Performance comparison on the pneumonia classification task.

Setting	Model	Large		Small				Client Average
		Client 1	Client 2	Client 3	Client 4	Client 5	Client 6	
Homo.	FedAvg	0.7862	0.7687	0.7464	0.7225	0.6685	0.6487	0.7235
	FedProx	0.8311	0.7996	0.7802	0.7648	0.6844	0.6605	0.7534
	Per-FedAvg	0.8451	0.8221	0.7878	0.7705	0.7002	0.6754	0.7669
	PFedMe	0.8523	0.8183	<u>0.7932</u>	0.7619	<u>0.7177</u>	<u>0.7163</u>	0.7766
	PFedBayes	<u>0.8569</u>	<u>0.8455</u>	0.7869	<u>0.7852</u>	0.7103	0.7085	<u>0.7822</u>
Hete.	FedMD	0.8456	0.8289	0.7905	0.7678	0.6948	0.6789	0.7678
	FedGH	0.8377	0.8163	0.7841	0.7612	0.6892	0.6647	0.7589
	FedKEAF	0.8301	0.8114	0.7857	0.7584	0.6867	0.6705	0.7571
	FCCL	0.8398	0.8024	0.7898	0.7608	0.6946	0.6680	0.7592
	FedHelp	0.9044	0.8846	0.8455	0.8032	0.8011	0.7645	0.8338
	(% imp.)	5.54% \uparrow	4.62% \uparrow	6.60% \uparrow	2.29% \uparrow	11.62% \uparrow	6.73% \uparrow	6.60% \uparrow

Table 4: Hyperparameter study on pneumonia classification task with chest x-ray dataset.

Hyperparameter	0.2	0.4	0.6
λ_J	0.8338	0.8406	0.8389
λ_B	0.8338	0.8311	0.8276

these improvements persist even when employing only the logits from public data as guidance in small client learning.

(2) **Communication Costs.** In this medical classification task, substituting the large model (ResNet110 with 1.73 million parameters) with the proxy model (ResNet20 with 0.27 million parameters) results in an approximately 84.39% reduction in communication costs per round. In summary, while the proposed model does slightly increase computational costs, the reduction in communication costs and substantial performance improvements strongly underscore its notable advantages.

4.3 Pneumonia Classification

4.3.1 Performance Comparison. We perform a binary classification evaluation for pneumonia using 5,863 chest x-ray images [44]. The dataset is divided among two large clients and four small clients, with the distribution of training and testing data as follows: 3,134/374, 1,048/124, 422/49, 317/37, 213/24, and 109/12, respectively. The experimental results are presented in Table 3. Similar patterns to those observed in Table 1 emerge, once again affirming the effectiveness of FedHelp.

4.3.2 Hyperparameter Analysis. We conduct a key hyperparameter study of our proposed approach, focusing on λ_J for the surrogate model in Eq. (3) and λ_B for the large model in Eq. (7). We keep all other settings consistent with Table 3 in the paper. The average accuracy is shown in Table 4. As the value of λ_J increases from 0.2 to 0.6, the performance initially improves and then declines. This trend may be due to the fact that appropriate utilization of public data enhances performance, but an over-reliance on it, at the expense of local data, can have a negative impact. Regarding λ_B , the performance declines slightly as it increases from 0.2 to 0.6. This

could be because a larger λ_B allows for more backward knowledge transfer from the surrogate model to the large model, which may be less quality than the knowledge passed from the large models to the surrogate models.

4.4 Public Dataset Selection

We also experimented to assess the sensitivity of public dataset selection. Initially, we fine-tuned the two foundation models on the NCT-CRC-HE-100K dataset, utilizing the last 10,000 images as the public data. The outcomes of the Fed-ISIC19 and pneumonia classification tasks are detailed in Table 5.

Compared to other heterogeneous baselines utilizing the same medical public data, our proposed model FedHelp demonstrates superior performance on each client and yields higher average results with the medical public data. When compared with the results using the CIFAR-100 dataset as the public data (refer to Table 1 and Table 3), the performance of FedHelp also experiences a marginal boost. This enhancement is attributed to the medical public data sharing more features similar to the local data, providing valuable knowledge that enhances the training of the small local client models. For baselines, the performance of FedMD and FedGH exhibits significant improvement when using public medical data. This enhancement is attributed to the similarity between the public data and private data, contributing to better consensus and thereby boosting local training.

Consequently, our experimental results underscore that our proposed approach is not heavily reliant on choosing the public dataset. However, incorporating medical data does have a slight positive impact on performance, particularly when local clients are engaged in medical-related tasks.

5 Medical Image Semantic Segmentation

The proposed FedHelp is a general framework that can be used for both medical image classification and segmentation tasks. In this section, we use two medical image semantic segmentation tasks – lung segmentation and brain mask segmentation – on both 2D and 3D images to validate the utility of our framework.

Table 5: Accuracy comparison with the medical public dataset (NCT-CRC-HE-100K).

Task	Setting	Model	Large			Small			Client Average
			Client 1	Client 2	Client 3	Client 4	Client 5	Client 6	
Melanoma	Homo.	FedAvg	0.4966	0.4820	0.4574	0.3955	0.3903	0.2345	0.4094
		FedProx	0.4895	0.4871	0.4612	0.4086	0.4015	0.2411	0.4148
		Per-FedAvg	0.5093	0.4903	0.4689	0.4126	0.4087	0.2456	0.4226
		PFedMe	0.5144	0.5066	0.4707	0.4233	0.4153	0.2508	0.4302
		PFedBayes	0.5365	0.5207	<u>0.4876</u>	0.4278	0.4222	0.2688	0.4439
	Hete.	FedMD	0.5377	0.5287	0.4644	0.4395	0.4207	<u>0.2932</u>	0.4474
		FedGH	<u>0.5409</u>	<u>0.5396</u>	0.4756	<u>0.4486</u>	<u>0.4303</u>	0.2864	<u>0.4536</u>
		FedKEAF	0.5261	0.5120	0.4733	0.4367	0.4289	0.2803	0.4429
		FCCL	0.5283	0.5197	0.4705	0.4304	0.4277	0.2784	0.4425
		FedHelp	0.5945	0.5644	0.5478	0.5375	0.4803	0.4132	0.5229
		(% imp.)	9.91% \uparrow	4.60% \uparrow	12.34% \uparrow	19.82% \uparrow	11.62% \uparrow	40.93% \uparrow	15.28% \uparrow
Task	Setting	Model	Large			Small			Client Average
			Client 1	Client 2	Client 3	Client 4	Client 5	Client 6	
Pneumonia	Homo.	FedAvg	0.7862	0.7687	0.7464	0.7225	0.6685	0.6487	0.7235
		FedProx	0.8311	0.7996	0.7802	0.7648	0.6844	0.6605	0.7534
		Per-FedAvg	0.8451	0.8221	0.7878	0.7705	0.7002	0.6754	0.7669
		PFedMe	0.8523	0.8183	0.7932	0.7619	<u>0.7177</u>	<u>0.7163</u>	0.7766
		PFedBayes	0.8569	<u>0.8455</u>	0.7869	<u>0.7852</u>	<u>0.7103</u>	<u>0.7085</u>	<u>0.7822</u>
	Hete.	FedMD	<u>0.8570</u>	0.8311	<u>0.8026</u>	0.7748	0.7109	0.6853	0.7770
		FedGH	0.8492	0.8264	0.7955	0.7693	0.7125	0.6768	0.7716
		FedKEAF	0.8389	0.8189	0.7893	0.7652	0.6804	0.6714	0.7607
		FCCL	0.8466	0.8175	0.8012	0.7707	0.7057	0.6891	0.7718
		FedHelp	0.9065	0.8881	0.8506	0.8017	0.8044	0.7667	0.8368
		(% imp.)	5.78% \uparrow	5.04% \uparrow	5.98% \uparrow	2.10% \uparrow	12.08% \uparrow	7.04% \uparrow	6.98% \uparrow

5.1 Datasets

The 2D lung segmentation dataset contains 704 images, and we distribute them to two large and one small clients with the following number of training/test data: 285/31, 285/31, and 65/7, respectively. The 3D brain T1 magnetic resonance images (MRIs) dataset is extracted from the Information extraction from Images (IXI) database. We still follow the data partition of Fed-IXI used by FLamby [25] and treat two clients as large and the third one as small. The number of training/testing images is 249/62, 145/36, and 59/15, respectively. The public dataset \mathcal{D}_p used in this experiment is the dermoscopic lesion image dataset in the 2016 ISIC Challenge, consisting of 900 binary mask images.

5.2 Baselines and Implementations

Except for the baselines used in Section 4, we also add a federated learning-based medical image segmentation approach FedSM [48] as a homogeneous baseline. We use MedSAM [20] as the foundation model API⁴ for segmentation tasks. We set $\lambda_R = 0.1$, $\lambda_J = 0.2$, $\lambda_F = 1$, $\lambda_B = 0.2$, $\beta_0 = 10$, and $\sigma = 5$. We use accuracy as the evaluation metric. We set the size of top-ranked classes Ω in Eq. (13) as 1 for the two segmentation tasks. The evaluation metrics are pixel accuracy and the Dice coefficient, following [11, 18, 48]. To ensure a fair comparison, an early stop mechanism is employed for

each model training, and we report the average performance of the latest 10 models before reaching convergence for all approaches.

5.3 Performance Analysis

Table 6 presents the experimental results for two segmentation tasks. It is evident that the proposed FedHelp consistently outperforms all baseline models. Notably, FedSM [48], designed specifically for medical image segmentation tasks, demonstrates superior performance compared to our baselines. Similar to the medical classification task findings, homogeneous models tend to outperform heterogeneous ones in other baselines. We also randomly select one input image from each client and visualize the segmentation results in Figure 4. These results reaffirm the effectiveness and generalization ability of FedHelp.

5.4 Ablation Study

Similar to the medical classification, we also conduct ablation studies to validate the utility of each proposed module. Since only one API, MedSAM [20], is used in this task, we keep FedHelp-only to validate the influence of foundation models. FedHelp_f, FedHelp_b, and FedHelp_s are kept to validate the proposed asymmetric dual knowledge distillation strategy. The observations of 2D lung segmentation (shown in Figure 5) are similar as discussed in Section 4.2.2.

⁴<https://github.com/bowang-lab/MedSAM>

Table 6: The segmentation task results.

Task	2D Lung Segmentation								3D Brain Mask Segmentation							
	Client 1		Client 2		Client 3		Client Avg		Client 1		Client 2		Client 3		Client Avg	
	Acc	DC	Acc	DC	Acc	DC	Acc	DC	Acc	DC	Acc	DC	Acc	DC	Acc	DC
FedAvg	0.8558	0.8316	0.8717	0.8505	0.8045	0.7720	0.8440	0.8180	0.7769	0.7520	0.7651	0.7317	0.7086	0.6869	0.7502	0.7235
FedProx	0.9034	0.8827	0.9145	0.9003	0.8696	0.8423	0.8958	0.8751	0.7926	0.7745	0.7955	0.7721	0.7357	0.7009	0.7746	0.7492
Per-FedAvg	0.9221	0.9057	0.9187	0.8976	0.8687	0.8493	0.9032	0.8842	0.8405	0.7987	<u>0.8168</u>	0.7865	0.7386	0.7086	<u>0.7986</u>	0.7646
PFedMe	<u>0.9277</u>	<u>0.9144</u>	0.9305	<u>0.9211</u>	0.8736	0.8625	0.9106	<u>0.8993</u>	0.8333	0.7932	0.8107	<u>0.7743</u>	<u>0.7499</u>	<u>0.7205</u>	0.7979	0.7627
PFedBayes	0.9146	0.8905	0.9216	0.9088	0.8604	<u>0.8688</u>	0.8989	<u>0.8894</u>	0.8475	0.8104	0.8155	<u>0.7927</u>	0.7214	0.7052	0.7948	<u>0.7694</u>
FedSM	0.9384	0.9076	<u>0.9351</u>	0.9046	<u>0.8751</u>	0.8663	<u>0.9162</u>	0.8928	<u>0.8488</u>	<u>0.8196</u>	0.8147	0.7784	0.7264	0.6963	0.7966	0.7637
FedMD	0.9203	0.9011	0.9257	0.9062	0.8679	0.8404	0.9046	0.8826	0.8388	0.8052	0.8122	0.7863	0.7259	0.7014	0.7923	0.7643
FedGH	0.9088	0.8848	0.9139	0.8968	0.8581	0.8315	0.8936	0.8710	0.8371	0.7989	0.8049	0.7730	0.7375	0.6937	0.7932	0.7552
FedKEAF	0.9105	0.8966	0.9216	0.9077	0.8525	0.8362	0.8949	0.8802	0.7902	0.7651	0.7845	0.7562	0.7223	0.6890	0.7657	0.7368
FCCL	0.9167	0.8905	0.9195	0.8944	0.8493	0.8320	0.8952	0.8723	0.8065	0.7678	0.7906	0.7654	0.7344	0.7107	0.7771	0.7479
FedHelp	0.9655	0.9378	0.9574	0.9297	0.9258	0.9026	0.9496	0.9234	0.8554	0.8248	0.8386	0.8295	0.7577	0.7389	0.8172	0.7977
(% imp.)	4.07% \uparrow	2.56% \uparrow	2.38% \uparrow	0.93% \uparrow	5.79% \uparrow	3.89% \uparrow	3.65% \uparrow	2.68% \uparrow	0.78% \uparrow	0.63% \uparrow	2.67% \uparrow	4.64% \uparrow	1.04% \uparrow	2.55% \uparrow	2.33% \uparrow	3.68% \uparrow

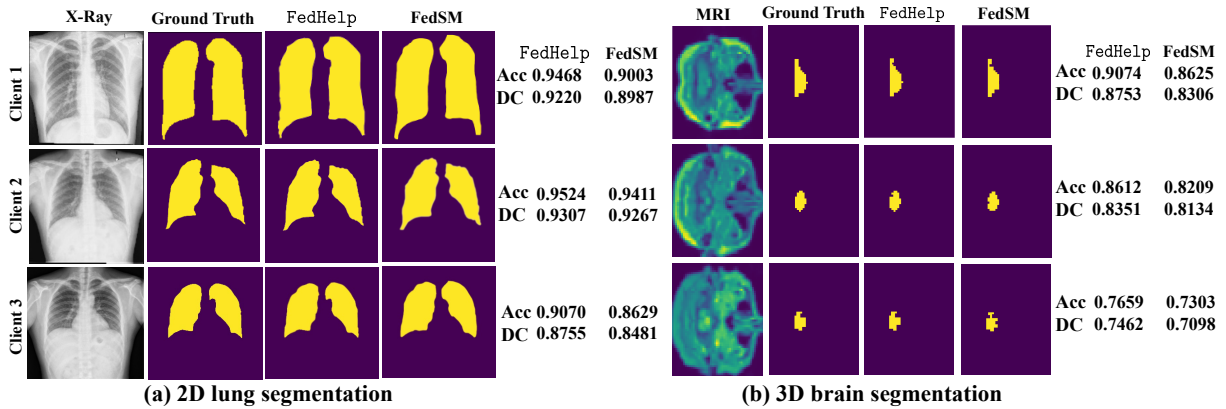


Figure 4: Visualization of 2D and 3D segmentation tasks.

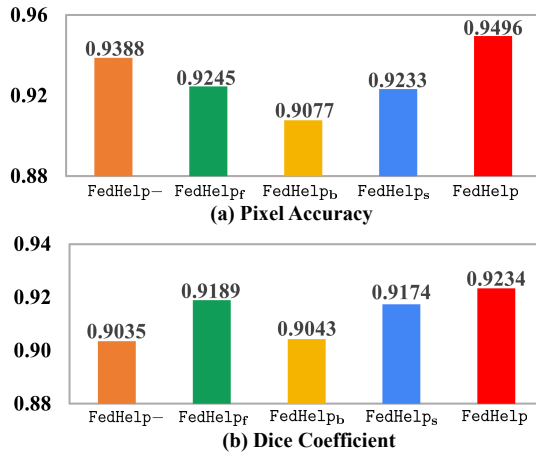


Figure 5: Ablation study results on segmentation task.

6 Conclusion

This paper addresses the challenge of geographic health disparities in underserved regions with the aim of enhancing healthcare quality, by employing advanced federated learning techniques. We introduce a novel framework, named FedHelp, which harnesses

the capabilities of foundation models to mitigate data insufficiency issues in underserved regions. Additionally, we propose a novel asymmetric dual knowledge distillation strategy to address the asymmetrical reciprocity among clients. Our experiments encompass both medical image classification (binary and multi-class labels) and segmentation tasks (2D and 3D). The experimental results confirm the effectiveness and utility of the proposed FedHelp, demonstrating its potential to ameliorate geographic health disparities. We are confident that this work will not only yield substantial benefits within the medical domain but will also deliver great value to businesses.

Acknowledgements

The authors thank the anonymous referees for their valuable comments and helpful suggestions. This work is partially supported by the National Science Foundation under Grant No. 2238275 and 2348541.

References

- [1] Dumilah Ayuningtyas, Dwi Hapsari, Rika Rachmalina, Vilda Amir, Riani Rachmawati, and Dian Kusuma. 2022. Geographic and socioeconomic disparity in child undernutrition across 514 districts in Indonesia. *Nutrients* 14, 4 (2022), 843.
- [2] Liwei Che, Jiaqi Wang, Yao Zhou, and Fenglong Ma. 2023. Multimodal federated learning: A survey. *Sensors* 23, 15 (2023), 6986.

- [3] Noel CF Codella, David Gutman, M Emre Celebi, Brian Helba, Michael A Marchetti, Stephen W Dusza, Aadi Kalloo, Konstantinos Liopyris, Nabin Mishra, Harald Kittler, et al. 2018. Skin lesion analysis toward melanoma detection: A challenge at the 2017 international symposium on biomedical imaging (isbi), hosted by the international skin imaging collaboration (isic). In *2018 IEEE 15th international symposium on biomedical imaging (ISBI 2018)*. IEEE, 168–172.
- [4] Nathan J Doogan, Megan E Roberts, Mary Ellen Wewers, Erin R Tanenbaum, Elizabeth A Mumford, and Frances A Stillman. 2018. Validation of a new continuous geographic isolation scale: A tool for rural health disparities research. *Social Science & Medicine* 215 (2018), 123–132.
- [5] Alexey Dosovitskiy, Lucas Beyer, Alexander Kolesnikov, Dirk Weissenborn, Xi-aohua Zhai, Thomas Unterthiner, Mostafa Dehghani, Matthias Minderer, Georg Heigold, Sylvain Gelly, et al. 2020. An image is worth 16x16 words: Transformers for image recognition at scale. *arXiv preprint arXiv:2010.11929* (2020).
- [6] Alireza Fallah, Aryan Mokhtari, and Asuman Ozdaglar. 2020. Personalized federated learning with theoretical guarantees: A model-agnostic meta-learning approach. *Advances in Neural Information Processing Systems* 33 (2020), 3557–3568.
- [7] Geoffrey Hinton, Oriol Vinyals, and Jeff Dean. 2015. Distilling the knowledge in a neural network. *arXiv preprint arXiv:1503.02531* (2015).
- [8] Wenke Huang, Mang Ye, and Bo Du. 2022. Learn from others and be yourself in heterogeneous federated learning. In *Proceedings of the IEEE/CVF Conference on Computer Vision and Pattern Recognition*. 10143–10153.
- [9] Fatih Ilhan, Gong Su, and Ling Liu. 2023. ScaleFL: Resource-Adaptive Federated Learning With Heterogeneous Clients. In *Proceedings of the IEEE/CVF Conference on Computer Vision and Pattern Recognition*. 24532–24541.
- [10] Hirofumi Inaguma, Tatsuya Kawahara, and Shinji Watanabe. 2021. Source and Target Bidirectional Knowledge Distillation for End-to-end Speech Translation. In *2021 Conference of the North American Chapter of the Association for Computational Linguistics: Human Language Technologies, NAACL-HLT 2021*. Association for Computational Linguistics (ACL), 1872–1881.
- [11] Meirui Jiang, Holger R Roth, Wenqi Li, Dong Yang, Can Zhao, Vishwesh Nath, Daguang Xu, Qi Dou, and Ziyue Xu. 2023. Fair Federated Medical Image Segmentation via Client Contribution Estimation. In *Proceedings of the IEEE/CVF Conference on Computer Vision and Pattern Recognition*. 16302–16311.
- [12] Shivam Kalra, Junfeng Wen, Jesse C Cresswell, Maksims Volkovs, and HR Tizhoosh. 2023. Decentralized federated learning through proxy model sharing. *Nature communications* 14, 1 (2023), 2899.
- [13] Alex Krizhevsky, Geoffrey Hinton, et al. 2009. Learning multiple layers of features from tiny images. (2009).
- [14] Wonbin Kweon, SeongKu Kang, and Hwanjo Yu. 2021. Bidirectional distillation for top-K recommender system. In *Proceedings of the Web Conference 2021*. 3861–3871.
- [15] Daliang Li and Junpu Wang. 2019. Fedmd: Heterogenous federated learning via model distillation. *arXiv preprint arXiv:1910.03581* (2019).
- [16] Qinbin Li, Bingsheng He, and Dawn Song. 2021. Model-contrastive federated learning. In *Proceedings of the IEEE/CVF conference on computer vision and pattern recognition*. 10713–10722.
- [17] Tian Li, Amit Kumar Sahu, Manzil Zaheer, Maziar Sanjabi, Ameet Talwalkar, and Virginia Smith. 2020. Federated optimization in heterogeneous networks. *Proceedings of Machine learning and systems* 2 (2020), 429–450.
- [18] Quande Liu, Cheng Chen, Jing Qin, Qi Dou, and Pheng-Ann Heng. 2021. Feddg: Federated domain generalization on medical image segmentation via episodic learning in continuous frequency space. In *Proceedings of the IEEE/CVF Conference on Computer Vision and Pattern Recognition*. 1013–1023.
- [19] Ruixuan Liu, Fangzhao Wu, Chuhan Wu, Yanlin Wang, Lingjuan Lyu, Hong Chen, and Xing Xie. 2022. No one left behind: Inclusive federated learning over heterogeneous devices. In *Proceedings of the 28th ACM SIGKDD Conference on Knowledge Discovery and Data Mining*. 3398–3406.
- [20] Jun Ma, Yuting He, Feifei Li, Lin Han, Chenyu You, and Bo Wang. 2023. Segment Anything in Medical Images. *arXiv preprint arXiv:2304.12306* (2023).
- [21] Xiaosong Ma, Jie Zhang, Song Guo, and Wenchao Xu. 2022. Layer-wise model aggregation for personalized federated learning. In *Proceedings of the IEEE/CVF conference on computer vision and pattern recognition*. 10092–10101.
- [22] Neil J MacKinnon, Vanessa Emery, Jennifer Waller, Brittany Ange, Preshit Ambade, Munira Gunja, and Emma Watson. 2023. Mapping health disparities in 11 high-income nations. *JAMA network open* 6, 7 (2023), e2322310–e2322310.
- [23] Brendan McMahan, Eider Moore, Daniel Ramage, Seth Hampson, and Blaise Agüera y Arcas. 2017. Communication-efficient learning of deep networks from decentralized data. In *Artificial intelligence and statistics*. PMLR, 1273–1282.
- [24] Matias Mendieta, Taojiannan Yang, Pu Wang, Minwoo Lee, Zhengming Ding, and Chen Chen. 2022. Local learning matters: Rethinking data heterogeneity in federated learning. In *Proceedings of the IEEE/CVF Conference on Computer Vision and Pattern Recognition*. 8397–8406.
- [25] Jean Ogier du Terrail, Samy-Safwan Ayed, Edwige Cyffers, Felix Grimberg, Chaoyang He, Regis Loeb, Paul Mangold, Tanguy Marchand, Othmane Marfoq, Erum Mushtaq, et al. 2022. FLamy: Datasets and Benchmarks for Cross-Silo Federated Learning in Realistic Healthcare Settings. *Advances in Neural Information Processing Systems* 35 (2022), 5315–5334.
- [26] Peihan Qi, Xiaoyu Zhou, Yuanlei Ding, Zhengyu Zhang, Shilian Zheng, and Zan Li. 2022. Fedbkd: Heterogenous federated learning via bidirectional knowledge distillation for modulation classification in iot-edge system. *IEEE Journal of Selected Topics in Signal Processing* 17, 1 (2022), 189–204.
- [27] Alec Radford, Jong Wook Kim, Chris Hallacy, Aditya Ramesh, Gabriel Goh, Sandhini Agarwal, Girish Sastry, Amanda Askell, Pamela Mishkin, Jack Clark, et al. 2021. Learning transferable visual models from natural language supervision. In *International conference on machine learning*. PMLR, 8748–8763.
- [28] Sashank Reddi, Rama Kumar Pasumarthi, Aditya Menon, Ankit Singh Rawat, Felix Yu, Seungyeon Kim, Andreas Veit, and Sanjiv Kumar. 2021. Rankdistil: Knowledge distillation for ranking. In *International Conference on Artificial Intelligence and Statistics*. PMLR, 2368–2376.
- [29] Olaf Ronneberger, Philipp Fischer, and Thomas Brox. 2015. U-net: Convolutional networks for biomedical image segmentation. In *Medical Image Computing and Computer-Assisted Intervention—MICCAI 2015: 18th International Conference, Munich, Germany, October 5–9, 2015, Proceedings, Part III* 18. Springer, 234–241.
- [30] Jennifer Prah Ruger and Hak-Ju Kim. 2006. Global health inequalities: an international comparison. *Journal of epidemiology & community health* 60, 11 (2006), 928–936.
- [31] Ertong Shang, Hui Liu, Zhuo Yang, Junzhao Du, and Yiming Ge. 2023. FedBiKD: Federated Bidirectional Knowledge Distillation for Distracted Driving Detection. *IEEE Internet of Things Journal* (2023).
- [32] Yiqing Shen, Yuyin Zhou, and Lequan Yu. 2022. Cd2-pfed: Cyclic distillation-guided channel decoupling for model personalization in federated learning. In *Proceedings of the IEEE/CVF Conference on Computer Vision and Pattern Recognition*. 10041–10050.
- [33] Dianbo Sui, Yubo Chen, Jun Zhao, Yantao Jia, Yuantao Xie, and Weijian Sun. 2020. Feded: Federated learning via ensemble distillation for medical relation extraction. In *Proceedings of the 2020 conference on empirical methods in natural language processing (EMNLP)*. 2118–2128.
- [34] Canh T Dinh, Nguyen Tran, and Josh Nguyen. 2020. Personalized federated learning with moreau envelopes. *Advances in Neural Information Processing Systems* 33 (2020), 21394–21405.
- [35] Minxue Tang, Xuefei Ning, Yitu Wang, Jingwei Sun, Yu Wang, Hai Li, and Yiran Chen. 2022. FedCor: Correlation-based active client selection strategy for heterogeneous federated learning. In *Proceedings of the IEEE/CVF Conference on Computer Vision and Pattern Recognition*. 10102–10111.
- [36] Philipp Tschandl, Cliff Rosendahl, and Harald Kittler. 2018. The HAM10000 dataset, a large collection of multi-source dermatoscopic images of common pigmented skin lesions. *Scientific data* 5, 1 (2018), 1–9.
- [37] Jiaqi Wang, Qi Li, Lingjuan Lyu, and Fenglong Ma. 2024. pFedClub: Controllable Heterogeneous Model Aggregation for Personalized Federated Learning. In *The Thirty-eighth Annual Conference on Neural Information Processing Systems*.
- [38] Jiaqi Wang and Fenglong Ma. 2023. Federated learning for rare disease detection: a survey. *Rare Disease and Orphan Drugs Journal* 2 (2023), 22.
- [39] Jiaqi Wang, Cheng Qian, Suhan Cui, Lucas Glass, and Fenglong Ma. 2022. Towards federated covid-19 vaccine side effect prediction. In *Joint European Conference on Machine Learning and Knowledge Discovery in Databases*. Springer, 437–452.
- [40] Jiaqi Wang, Xiaochen Wang, Lingjuan Lyu, Jinghui Chen, and Fenglong Ma. 2024. FEDMEKI: A Benchmark for Scaling Medical Foundation Models via Federated Knowledge Injection. In *The Thirty-eighth Annual Conference on Neural Information Processing Systems*.
- [41] Jiaqi Wang, Xingyi Yang, Suhan Cui, Liwei Che, Lingjuan Lyu, Dongkuan Xu, and Fenglong Ma. 2023. Towards Personalized Federated Learning via Heterogeneous Model Reassembly. In *Thirty-seventh Conference on Neural Information Processing Systems*.
- [42] Jiaqi Wang, Xingyi Yang, Suhan Cui, Liwei Che, Lingjuan Lyu, Dongkuan DK Xu, and Fenglong Ma. 2024. Towards personalized federated learning via heterogeneous model reassembly. *Advances in Neural Information Processing Systems* 36 (2024).
- [43] Jiaqi Wang, Chenxu Zhao, Lingjuan Lyu, Quanzeng You, Mengdi Huai, and Fenglong Ma. 2024. Bridging Model Heterogeneity in Federated Learning via Uncertainty-based Asymmetrical Reciprocity Learning. In *Proceedings of the 41st International Conference on Machine Learning (Proceedings of Machine Learning Research, Vol. 235)*, Ruslan Salakhutdinov, Zico Kolter, Katherine Heller, Adrian Weller, Nuria Oliver, Jonathan Scarlett, and Felix Berkenkamp (Eds.). PMLR, 52290–52308. <https://proceedings.mlr.press/v235/wang24cs.html>
- [44] Xiaosong Wang, Yifan Peng, Le Lu, Zhiyong Lu, Mohammadhadi Bagheri, and Ronald M Summers. 2017. Chestx-ray8: Hospital-scale chest x-ray database and benchmarks on weakly-supervised classification and localization of common thorax diseases. In *Proceedings of the IEEE conference on computer vision and pattern recognition*. 2097–2106.
- [45] Xiaochen Wang, Jiaqi Wang, Houping Xiao, Jinghui Chen, and Fenglong Ma. 2024. FEDKIM: Adaptive Federated Knowledge Injection into Medical Foundation Models. In *Proceedings of the 2024 Conference on Empirical Methods in Natural Language Processing*, Yaser Al-Onaizan, Mohit Bansal, and Yun-Nung

- Chen (Eds.). Association for Computational Linguistics, Miami, Florida, USA, 8141–8154. <https://doi.org/10.18653/v1/2024.emnlp-main.464>
- [46] Yanping Wang, Jun Zhu, Chunhua He, Xiaohong Li, Lei Miao, and Juan Liang. 2012. Geographical disparities of infant mortality in rural China. *Archives of Disease in Childhood-Fetal and Neonatal Edition* 97, 4 (2012), F285–F290.
- [47] Jennifer Weisent, Barton Rohrbach, John R Dunn, and Agricola Odoi. 2012. Socioeconomic determinants of geographic disparities in campylobacteriosis risk: a comparison of global and local modeling approaches. *International journal of health geographics* 11 (2012), 1–16.
- [48] An Xu, Wenqi Li, Pengfei Guo, Dong Yang, Holger R Roth, Ali Hatamizadeh, Can Zhao, Daguang Xu, Heng Huang, and Ziyue Xu. 2022. Closing the generalization gap of cross-silo federated medical image segmentation. In *Proceedings of the IEEE/CVF Conference on Computer Vision and Pattern Recognition*. 20866–20875.
- [49] Liping Yi, Gang Wang, Xiaoguang Liu, Zhuhan Shi, and Han Yu. 2023. FedGH: Heterogeneous Federated Learning with Generalized Global Header. *arXiv preprint arXiv:2303.13137* (2023).
- [50] Sixing Yu, Wei Qian, and Ali Jannesari. 2022. Resource-aware Federated Learning using Knowledge Extraction and Multi-model Fusion. *arXiv preprint arXiv:2208.07978* (2022).
- [51] Huaao Zhang, Shigui Qiu, and Shilong Wu. 2021. Dual knowledge distillation for bidirectional neural machine translation. In *2021 International Joint Conference on Neural Networks (IJCNN)*. IEEE, 1–7.
- [52] Xu Zhang, Yinchuan Li, Wenpeng Li, Kaiyang Guo, and Yunfeng Shao. 2022. Personalized federated learning via variational bayesian inference. In *International Conference on Machine Learning*. PMLR, 26293–26310.
- [53] Yao Zhou, Jun Wu, Haixun Wang, and Jingrui He. 2022. Adversarial robustness through bias variance decomposition: A new perspective for federated learning. In *Proceedings of the 31st ACM International Conference on Information & Knowledge Management*. 2753–2762.
- [54] Weiming Zhuang, Chen Chen, and Lingjuan Lyu. 2023. When foundation model meets federated learning: Motivations, challenges, and future directions. *arXiv preprint arXiv:2306.15546* (2023).
- [55] Yimeng Zhuang and Mei Tu. 2023. Pretrained Bidirectional Distillation for Machine Translation. In *Proceedings of the 61st Annual Meeting of the Association for Computational Linguistics (Volume 1: Long Papers)*. Association for Computational Linguistics, Toronto, Canada, 1132–1145. <https://doi.org/10.18653/v1/2023.acl-long.63>

Appendix

A. Medical Image Semantic Segmentation

Here, we provide the details of FedHe1p for the medical image segmentation task, which is similar to the medical image classification task but uses different loss functions for small and large client updates.

For the **small client training**, we still use APIs to obtain the pixel-level distributions $\{F_m(\mathbf{x}_{p,q})\}_{q=1}^{Q_p}$, where Q_p is the number of pixels in \mathbf{x}_p . After that, we can have the surrogate segmentation model training loss as follows:

$$\mathcal{R}_i^s = \sum_{p=1}^P \sum_{q=1}^{Q_p} \beta_{p,q} [\text{CE}(\hat{\mathbf{w}}_i^s(\mathbf{x}_{p,q}), Y_{p,q})] \quad (8)$$

$$+ \lambda_R \text{KL} \left(\sum_{m=1}^M \alpha_{i,p}^m F_m(\mathbf{x}_{p,q}) \parallel \hat{\mathbf{w}}_i^s(\mathbf{x}_{p,q}) \right), \quad (9)$$

where $\beta_{p,q}$ is a weight map to distinguish the importance of pixels in the training. Following U-Net [29], we pre-compute the weight map as follows:

$$\beta_{p,q} = \beta_{p,q}^c + \beta_o * \exp\left(-\frac{(d_1(\mathbf{x}_{p,q}) + d_2(\mathbf{x}_{p,q}))^2}{2\sigma^2}\right), \quad (10)$$

where $\beta_{p,q}^c$ is the weight map to balance the class frequencies. d_1 and d_2 are the distances to the border of the nearest and the second nearest cell, respectively. β_o and σ are hyperparameters. FedHe1p then uses the private data to train the segmentation model using

the loss as Eq. (3):

$$\mathcal{L}_i^s = \sum_{k=1}^{K_i^s} \sum_{q=1}^{Q_k^s} \beta_{k,q}^{s,i} \text{CE}(\mathbf{w}_i^s(\mathbf{x}_{k,q}^{s,i}), \mathbf{y}_{k,q}^{s,i}), \quad (11)$$

where $\beta_{k,q}^{s,i}$ is the weight map that can be obtained with Eq. (10).

For the **large client training**, we still conduct the pixel-level classification via the proposed asymmetrical dual knowledge distillation. In the forward distillation, we still use traditional knowledge distillation for each pixel with the loss:

$$\overrightarrow{\mathcal{KD}}_j^l = \sum_{k=1}^{K_j^l} \sum_{q=1}^{Q_k^l} \text{KL}(\mathbf{w}_j^l(\mathbf{x}_{k,q}^{l,j}) \parallel \tilde{\mathbf{w}}_j^l(\mathbf{x}_{k,q}^{l,j})). \quad (12)$$

The backward distillation is based on the top-ranked classes of each pixel as follows:

$$\overleftarrow{\mathcal{KD}}_j^l = - \sum_{k=1}^{K_j^l} \sum_{q=1}^{Q_k^l} \sum_{r \in \Omega} \log\left(\frac{\exp(\mathbf{w}_j^l(\mathbf{x}_{k,q}^{l,j})[r])}{\Phi}\right), \quad (13)$$

$$\Phi = \sum_{u \in \Omega} \exp(\mathbf{w}_j^l(\mathbf{x}_{k,q}^{l,j})[u]) + \sum_{v \in \Omega'} \exp(\mathbf{w}_j^l(\mathbf{x}_{k,q}^{l,j})[v]). \quad (14)$$

Finally, following Eq. (7), we combine the cross-entropy loss \mathcal{L}_j^l similar to Eq. (11), the forward loss $\overrightarrow{\mathcal{KD}}_j^l$, and the backward loss $\overleftarrow{\mathcal{KD}}_j^l$, to train the segmentation models.

B. Algorithm Flow

To provide a clear illustration of FedHe1p, we outline the algorithmic flow in Algorithm 1. Notably, (1) we consolidate medical image classification and segmentation within Algorithm 1; (2) the small client update and large client update can be executed in parallel; and (3) obtaining logits of public data by querying the foundation models can be performed before model training, as they remain constant. Importantly, FedHe1p optimizes communication costs by exclusively uploading and downloading small models, as indicated in lines 23 and 26.

C. Baselines

In the **homogeneous** setting, we use the following approaches as the baselines:

- FedAvg [23] trains a global model by averaging model updates from multiple decentralized clients, without sharing local data. Each client trains locally and sends updates to a central server, which averages these to improve the global model. The updated global model is then shared with all participants for further local training.
- FedProx [17] addresses the heterogeneity challenge in federated learning by generalizing and re-parameterizing FedAvg.
- Per-FedAvg [6] treats the global model as the initialization for the local client training and targets searching an optimal model initialization for each client model personalization within a few steps of local updates.
- PFedMe [34] utilizes Moreau envelopes for client loss functions to guide the local model personalized learning, which decouples personalized model learning from global model learning.

Algorithm 1: Algorithm Flow of FedHelp.

Input: Small and large client data $\{\mathcal{D}_1^s, \dots, \mathcal{D}_{N_s}^s\}$ and $\{\mathcal{D}_1^l, \dots, \mathcal{D}_{N_l}^l\}$, public data \mathcal{D}_p , communication rounds T , foundation models $\{F_1, \dots, F_M\}$.

- 1 Initialize client models $\{\mathbf{w}_{1,0}^s, \dots, \mathbf{w}_{N_s,0}^s\}$ and $\{\mathbf{w}_{1,0}^l, \dots, \mathbf{w}_{N_l,0}^l\}$
- 2 Query M APIs from foundation models $\{F_1, \dots, F_M\}$ with public data \mathcal{D}_p ;
- 3 **for** each communication round $t = 1, 2, \dots, T$ **do**
- 4 **ClientUpdate:**
- 5 # Small client update
- 6 **for** $i \in [1, \dots, N_s]$ **do**
- 7 **if** $t > 1$ **then**
- 8 $\mathbf{w}_{i,t}^s = \mathbf{w}_{i,t-1}^g$;
- 9 **end**
- 10 Calculate $\mathcal{R}_{i,t}^s$ via Eq. (1)/Eq. (8) using the public data \mathcal{D}_p ;
- 11 Calculate $\mathcal{L}_{i,t}^s$ via Eq. (2)/Eq. (11) using private data \mathcal{D}_i ;
- 12 Jointly optimize $\mathcal{R}_{i,t}^s$ and $\mathcal{L}_{i,t}^s$ by minimizing $\mathcal{J}_{i,t}^s$ via Eq. (3);
- 13 **end**
- 14 # Large client update
- 15 **for** $j \in [1, \dots, N_l]$ **do**
- 16 **if** $t > 1$ **then**
- 17 $\hat{\mathbf{w}}_{j,t}^l = \mathbf{w}_{j,t-1}^g$;
- 18 **end**
- 19 Calculate $\overrightarrow{\mathcal{KD}}_{j,t}^l$ via Eq. (4)/Eq. (12);
- 20 Calculate $\overleftarrow{\mathcal{KD}}_{j,t}^l$ via Eq. (5)/Eq. (13);
- 21 Update $\mathcal{G}_{j,t}^l$ by minimizing $\mathcal{G}_{j,t}^l$ via Eq. (7);
- 22 **end**
- 23 Upload $\{\mathbf{w}_{1,t}^s, \dots, \mathbf{w}_{N_s,t}^s\}$ and $\{\hat{\mathbf{w}}_{1,t}^l, \dots, \hat{\mathbf{w}}_{N_l,t}^l\}$ to the server;
- 24 **ServerUpdate:**
- 25 Obtain the aggregated model \mathbf{w}_t^g via FedAvg;
- 26 Distribute the aggregated model \mathbf{w}_t^g back to clients.
- 27 **end**

- PFedBayes [52] uses Bayesian variational inference to achieve personalized federated learning, which balances the data reconstruction error and KL divergence between local and global distributions during local updates.
- FedSM [48] is designed for the medical segmentation task in federated learning, which addresses the generalization gap caused by client drift from non-iid data distribution.

We use the following **heterogeneous** baselines:

- FedMD [15] employs transfer learning and knowledge distillation, utilizing labeled public data on the server. Each client is required to train their local model using both public and private datasets. Subsequently, the clients transmit their class scores from the public dataset to the server, which then computes a consensus and sends it back to the clients for updating their models locally.
- FedGH [49] allows clients to use individual feature extractors while sharing a uniform global header. Specifically, clients train their local models on personal data and send back both the representations and labels for each category to the server, facilitating the update of the global header. Following this, clients substitute their personal headers with the updated global header for making inferences.
- FCCL [8] aims to tackle heterogeneity in federated learning by creating a cross-correlation matrix using unlabeled public data, aiding domain shift adaptation. It utilizes knowledge distillation in local updates to combat catastrophic forgetting while maintaining privacy. Clients send logits to the server for aggregation and then use the consensus logits to steer their local training processes.
- FedKEMF [50] focuses on training diverse local models, facilitating effective knowledge integration, and implementing resource-conscious models. Clients transmit their network models to the server for a comprehensive knowledge distillation process. Subsequently, the server generates personalized models for each client and redistributes these for local updates.

D. Dataset Repository

We use the following datasets in our experiments:

- Fed-ISIC19: https://github.com/owkin/FLamby/tree/main/flamby/datasets/fed_isic2019.
- Pneumonia chest x-ray images: <https://www.kaggle.com/datasets/paultimothymooney/chest-xray-pneumonia/data>
- 2D lung segmentation dataset: <https://www.kaggle.com/datasets/nikhilpandey360/chest-xray-masks-and-labels/>
- Information extraction from Images (IXI) database: <https://brain-development.org/ixi-dataset>
- 3D Fed-IXI: https://github.com/owkin/FLamby/tree/main/flamby/datasets/fed_ixi
- Dermoscopic lesion image dataset: https://isic-challenge-data.s3.amazonaws.com/2016/ISBI2016_ISIC_Part1_Training_Data.zip
- NCT-CR-HE-100K: <https://paperswithcode.com/dataset/nct-crc-he-100k>